Proc. Natl. Acad. Sci. USA
Vol. 91, pp. 10335–10339, October 1994
Cell Biology

Paneth cell differentiation in the developing intestine of normal and transgenic mice

LYNN BRY*, PER FALK*, KENNETH HUTTNER†, ANDRE OUELLETTE‡, TORE MIDTVEDT§, AND JEFFREY I. GORDON*

*Department of Molecular Biology and Pharmacology, Washington University School of Medicine, St. Louis, MO 63110; †Department of Genetics, Harvard Medical School, Boston, MA 02115; ‡Department of Surgery, Harvard Medical School and Surgical Services, Massachusetts General Hospital, and Shriners Burns Institute, Boston, MA 02114; and §Laboratory of Medical Microbial Ecology, Karolinska Institute, S-171 77, Stockholm, Sweden

Communicated by David M. Kipnis, June 20, 1994

ABSTRACT **Paneth cells represent one of the four major epithelial lineages in the mouse small intestine. It is the only lineage that migrates downward from the stem-cell zone located in the lower portion of the crypt of Lieberkühn to the crypt base. Mature Paneth cells release growth factors, digestive enzymes, and antimicrobial peptides from their apical secretory granules. Some of these factors may affect the crypt stem cell, its transit-cell descendants, differentiating villus-associated epithelial lineages, and/or the gut microflora. We used single and multilabel immunocytochemical methods to study Paneth cell differentiation during and after completion of gut morphogenesis in normal, gnotobiotic, and transgenic mice as well as in intestinal isografts. This lineage emerges coincident with cytodifferentiation of the fetal small intestinal endoderm, formation of crypts from an intervillus epithelium, and establishment of a stem-cell hierarchy. The initial differentiation program involves sequential expression of cryptdins, a phospholipase A_2 (enhancing factor), and lysozyme. A dramatic increase in Paneth cell number per crypt occurs during postnatal days 14–28, when crypts proliferate by fission. Accumulation of fucosylated and sialylated glycoconjugates during this period represents the final evolution of the lineage's differentiation program. Establishment of this lineage is not dependent upon instructive interactions from the microflora. Transgenic mice containing nucleotides −6500 to +34 of the Paneth cell-specific mouse cryptdin 2 gene linked to the human growth hormone gene beginning at its nucleotide +3 inappropriately express human growth hormone in a large population of proliferating and nonproliferating cells in the intervillus epithelium up to postnatal day 5. Transgene expression subsequently becomes restricted to the Paneth cell lineage in the developing crypt. Cryptdin 2 nucleotides −6500 to +34 should be a useful marker of crypt morphogenesis and a valuable tool for conducting gain-of-function or loss-of-function experiments in Paneth cells.**

The four principal epithelial cell lineages of the adult mouse small intestine derive from a multipotent stem cell located near the base of crypts of Lieberkühn (1). The stem cell's immediate descendants undergo several rounds of cell division in the mid-portion of the crypt. After exiting the cell cycle, members of the goblet, enteroendocrine, and enterocytic lineages complete their differentiation during a 2- to 5-day upward migration to the apical extrusion zone of associated villi. Paneth cells differentiate during a downward migration to the base of the crypt, where they reside for ≈20 days (2) before being removed by phagocytosis (3).

A variety of functions have been attributed to Paneth cells. These functions include modulation of the intestinal microflora and maintenance of mucosal defense barriers through production of antimicrobial peptides (cryptdins, lysozyme). The location of Paneth cells at the crypt base, combined with their production of growth factors and other regulatory molecules (4–6), suggests that they may also contribute to the stem-cell niche through short-circuit paracrine loops and/or regulate the proliferation and differentiation programs of other cell lineages.

One way of examining Paneth cell function is to study the differentiation program of this lineage during gut development. Morphogenesis of the mouse small intestinal epithelium is not completed until the end of the third postnatal week. A pseudostratified endoderm undergoes conversion to a monolayer overlying nascent villi in a morphologic "wave" of cytodifferentiation. This wave moves from the duodenum to the ileum from embryonic day 15 (E15) through E19. Crypts form from an intervillus epithelium during the first two postnatal weeks (7). Crypt number increases rapidly between the second and third postnatal week through crypt fission (7). Analyses of mouse aggregation chimeras indicate that the perinatal mouse gut contains a polyclonal intervillus epithelium, supplied by stem cells with multiple genotypes (8). A process of cell selection occurs during crypt morphogenesis, yielding monoclonal crypts by postnatal day 14 (P14). An adult mouse crypt appears to be supplied either by a single slowly dividing master stem cell and its more rapidly cycling transit-cell descendants (the stem-cell pedigree concept) or by several equivalent stem cells with similar cycling times and probabilities for self-maintenance (9).

We have examined the Paneth cell lineage from E15 to P42 in germ-free, ex-germ-free, and conventional mice and in intestinal isografts. The results of these studies form a basis for interpreting the significance of the pattern of expression of a mouse cryptdin 2/human growth hormone (hGH) transgene in several pedigrees of mice.

MATERIALS AND METHODS

Animals. FVB/N mice were caged in microisolators and given autoclaved chow (Ralston Purina) ad libitum. Germ-free NMRI mice (10) were maintained in gnotobiotic isolator cages. Conventional NMRI animals were housed in a non-sterile but pathogen-free environment. Ex-germ-free NMRI mice were generated by removing P28 germ-free animals from their isolator cages and placing them in cages with conventional animals for 2 weeks. All NMRI mice were fed the same autoclaved chow. Germ-free and conventional NMRI mice were killed at P1, P5, P7, P10, P14, P21, P25, P28, and P42 (n = 5 mice per time point). Four FVB/N mice were

The publication costs of this article were defrayed in part by page charge payment. This article must therefore be hereby marked "*advertisement*" in accordance with 18 U.S.C. §1734 solely to indicate this fact.

Abbreviations: En, embryonic day n; Pn, postnatal day n; EF, enhancing factor; hGH, human growth hormone; FITC, fluorescein isothiocyanate; TRITC, tetramethylrhodamine isothiocyanate; AAA, *Anguilla anguilla* agglutinin; MAA, *Maackia amurensis* agglutinin; OPA, orange peel fungus agglutinin; UEA-1, *Ulex europaeus* agglutinin 1; P/T, phloxine/tartrazine.

killed at each of these time points. FVB/N litters were also examined at E10, E15, and E18. Four ex-germ-free mice were killed at P42. Animals were given an intraperitoneal injection of 5-bromo-2'-deoxyuridine (BrdUrd, 120 mg/kg) 2 hr prior to sacrifice to label cells in S phase.

Isografts. The gastrointestinal tracts of E15 FVB/N mice were removed. The entire small intestine and the colon from each donor were placed into paravertebral subcutaneous tunnels fashioned in P42 syngenic male or female recipients. Isografts were harvested 4–46 days after implantation. Since the gestation time of FVB/N mice is 19 days, an E15 isograft harvested 4 days after implantation was considered equivalent in age to the intact gut of an E19 animal.

Generation of Pedigrees of Cryptdin 2(−6500 to +34)/hGH(+3) Transgenic Mice. An 8.3-kb *Eco*RI fragment containing nt −6500 to +34 of the mouse cryptdin 2 gene (11) linked to nt +3 to +2150 of the hGH gene was microinjected into FVB/N oocytes. Tail DNAs from 72 liveborn mice were screened by PCR using primers that recognize the first exon of the hGH gene (11). Four founders were identified. Lines were established from each founder and maintained by crosses to nontransgenic littermates. Southern blot analysis revealed that lines 38, 57, and 61 had <10 copies of the transgene per haploid genome, whereas line 70 had 250 copies.

Single- and Multilabel Immunocytochemical Studies. The entire gastrointestinal tract was removed and fixed in phosphate-buffered 10% formalin or Bouin's solution (two to four mice per developmental time point). The small intestine was rolled up into a compact circle, placed in mounting agar (together with segments prepared from the stomach, proximal, mid, and distal colon). Tissues were then embedded in paraffin and sectioned (5–8 μm). Some slides were treated with Lugol's iodine solution prior to immunostaining. Methods for single and multilabel immunocytochemical staining have been described (12), as have the specificities and staining characteristics of a panel of polyclonal sera: rabbit anti-mouse cryptdin 1 [ref. 13; final dilution, 1:25 in phosphate-buffered saline (PBS)/blocking buffer (12)], rabbit anti-human lysozyme (Dako; 1:500), rabbit anti-mouse enhancing factor (EF) (1:5000; ref. 6), rabbit anti-rat intestinal fatty acid-binding protein (1:2000; ref. 12), goat anti-hGH (1:2000; ref. 12), and rabbit anti-rat sucrase–isomaltase (1:500; ref. 14). Antigen–antibody complexes were detected with immunogold/silver enhancement or with fluorescence-tagged secondary antibodies. Sections were also incubated with tetramethylrhodamine isothiocyanate (TRITC)- or fluorescein isothiocyanate (FITC)-labeled *Ulex europaeus* agglutinin 1 (UEA-1), orange peel fungus agglutinin (OPA), *Anguilla anguilla* agglutinin (AAA), or *Maackia amurensis* agglutinin (MAA) (15). The number of Paneth cells reacting with each antibody or lectin was determined in the proximal duodenum and distal ileum of the intact gut and in comparably aged isografts. Slides were randomly assigned a code to allow for objective analysis. One hundred to 150 well-oriented crypts were counted per gut segment for each time point (two intact intestines per time point and two or three E19, P3, P5, P7, P14, P21, P28, and P42 isografts).

Analyses of RNAs Prepared from Transgenic and Normal FVB/N Mouse Tissues. Total cellular RNA was prepared from 2-cm segments of duodenum, mid-jejunum, mid-ileum, cecum, and colon plus samples of stomach, pancreas, liver, lung, heart, brain, kidney, adrenal, testis, spleen, thymus, and skin. Blots of total cellular RNA were probed with a ^{32}P-labeled hGH DNA (11) or with a labeled cryptdin 2 cDNA (16). Reverse transcription–PCR was performed with recombinant *Tth* polymerase (Perkin–Elmer), 200 ng of total cellular RNA, and reaction conditions suggested by Perkin–Elmer. hGH mRNA was detected with 5'-AGGTGGCCTTTGACACCTACCAGG-3' and 5'-TCTGTTGTGTTTCCTCCCTGTTGG-3'. Primers 5'-TCTTCTTTTGCAACCTCTTG-3' and 5'-TTCTGCCCTTGTCCTACTGT-3' were used to identify cryptdin mRNAs [this primer pair is derived from sequences conserved in 17 intestinal defensins (16, 17)].

RESULTS AND DISCUSSION

Temporal and Spatial Map of the Appearance of the Paneth Cell Lineage During Intestinal Development. The duodenal-to-colonic axis of E10–P42 FVB/N mice was surveyed with a panel of antibodies and lectins previously reported to react with adult Paneth cells in this and other strains. Since intervillus epithelial cells in the late-gestation intestine are not cleared from the nascent crypt–villus axis until P10 (duodenum) or P14 (ileum) (7), the portion of our analysis spanning E15 to P10–14 provides information about the initial differentiation program of Paneth cells.

A general survey of cryptdin production in Paneth cells was conducted with a polyclonal antibody raised against residues 4–35 of one of the most abundant intestinal defensins, cryptdin 1 (13). This antibody reacts with purified cryptdins 1, 2, 3, and 6 in ELISAs (M. Selsted, personal communication). Cryptdin-positive cells first appear interspersed in the intervillus epithelium of E15 small intestine—i.e., on the day the gut endoderm is first converted to a monolayer. Cryptdin-positive goblet cells appear late in gestation. Some of these cells coexpress carbohydrates recognized by the fucose-specific lectin UEA-1 (Fig. 1*A*). At P1, cryptdin-positive goblet cells represent <10% of all goblet cells. The intervillus epithelium contains a larger population of cryptdin-positive cells that do not bind UEA-1 or incorporate BrdUrd (Fig. 1*B*). By P7, most cryptdin-positive cells have the morphologic appearance of Paneth cells, with apical secretory granules, although occasional goblet cells stain with the antibody. The number of crypts containing cryptdin-positive Paneth cells and the number of positive cells per crypt decrease progressively along the duodenal–ileal axis. By P14, the number of cryptdin-positive crypts in the proximal half of the FVB/N small intestine equals that in its distal half (77% of all crypts contain cryptdin-immunoreactive cells with an average of 1.4 positive cells per crypt). As crypt number increases throughout the small intestine due to crypt fission (P14 → P28), the number of cryptdin-positive crypts and cryptdin-producing Paneth cells per crypt also increases. These increases are greater in the distal than in the proximal half of the small intestine. The change in distribution of cryptdin-positive cells does not reflect an absolute reduction in their number in the duodenum and proximal jejunum but rather a relative augmentation in the distal jejunum and ileum (e.g., from an average of 1.7 cells per ileal crypt at P14 to 4.3 cells per ileal crypt at P28). By P42, >95% of all crypts per cross section of small intestine contain cryptdin-positive cells (average, 3.1 cells per duodenal crypt; 5 cells per ileal crypt). At P42, no cryptdin-positive goblet cells can be found in duodenal, jejunal, or ileal villi. Cryptdin-positive cells are not detectable in the surface epithelium or in the crypts of the cecum or colon of E15–P42 FVB/N mice.

The expression patterns of other Paneth cell products also support the notion that the emergence of this cell lineage along the duodenal–ileal axis coincides with crypt morphogenesis. EF, a phospholipase A_2 isolated based on its ability to enhance the binding of epidermal growth factor to its receptor, is a Paneth cell-specific marker in adult mice (18). EF-positive cells are not detectable until P7 in the FVB/N strain. By P14, the percentages of EF-positive crypts in the proximal (Fig. 1*C*) and distal small intestine are equal (74% versus 77% per cross section), although the number of EF-positive cells per positive crypt per cross section is slightly higher in the ileum. By P28, an adult cephalocaudal distribution of EF-producing Paneth cells is fully established.

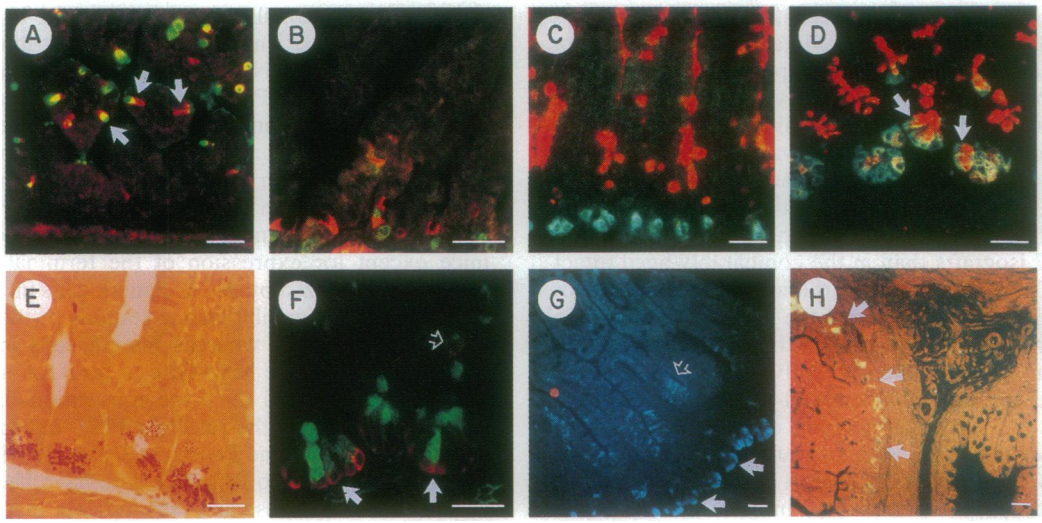

FIG. 1. Paneth cell differentiation in FVB/N mouse intestine and intestinal isografts. (*A*) Section of E18 proximal small intestine stained with rabbit anti-cryptdin 1 and indocarbocyanine-labeled donkey anti-rabbit sera plus FITC-conjugated UEA-1. The villi are seen in cross section above the intervillus epithelium, which is located at the bottom of the panel. Many cryptdin-positive cells (red) bind UEA-1 (red–yellow–green; arrows). (*B*) P1 distal small intestine stained for cryptdin as in *A*, plus goat anti-BrdUrd and FITC-labeled donkey anti-goat immunoglobulins. Villi have been sectioned along their basilar to apical axis. The cryptdin-positive cells (red), located in the intervillus epithelium at the bottom of the micrograph, do not incorporate BrdUrd (green), indicating that they are not proliferating. (*C*) P14 jejunum stained with rabbit anti-EF and immunogold-labeled goat anti-rabbit sera plus TRITC-conjugated UEA-1. EF-positive Paneth cells (turquoise, at the base of newly formed crypts) do not bind UEA-1 (red) at this stage of development. UEA-1-positive goblet cells are evident in the upper portions of the crypt and villus. (*D*) P28 jejunum stained as in *C*. EF-positive Paneth cells (turquoise) now demonstrate strong staining of their apical granules with UEA-1 (red; arrows). Goblet cells (red only; top) also bind UEA-1. (*E*) Phloxine/tartrazine (P/T) staining of Paneth cell granules (red) in P42 jejunal crypts. (*F*) P42 ileum stained with rabbit anti-human lysozyme and TRITC-labeled donkey anti-rabbit sera, plus FITC-conjugated MAA. A subset of lysozyme-positive Paneth cells (red, at the base of crypts) coexpress sialylated carbohydrate epitopes in their apical granules which are recognized by MAA (green; solid arrows). Open arrow points to a lysozyme-positive macrophage in the lamina propria. (*G*) Section of a P42 isograft stained as in *C* for EF. Paneth cells located in the base of crypts (lower right) contain immunoreactive EF (solid arrows). Open arrows point to villus-associated, EF-positive enterocytes. Our immunocytochemical methods cannot distinguish between anomalous transcription of the mouse EF gene in the enterocytic lineage or uptake of EF released from crypt-associated Paneth cells. EF-positive villus-associated enterocytes are also evident in P10–P28 isografts (data not shown). (*H*) P7 isograft stained for EF as in *C* and with rabbit anti-intestinal fatty acid-binding protein and TRITC-labeled donkey anti-rabbit sera. The section juxtaposes a proximal section of small intestine (left) with a more distal one (right). Paneth cells located at the base of crypts in the proximal section produce EF (white, arrows; the lower portion of villi are seen extending to the left margin). EF is not detectable in the distal section (right). (Bars = 25 μm.)

At no time is EF detectable in villus-associated epithelial cells (Fig. 1*D*) or in the epithelial cell lineages of the stomach and colon (data not shown). P/T is the most specific histochemical stain available for detecting the Paneth cell's apical secretory apparatus. P/T-positive Paneth cells can be first detected at the base of nascent proximal small intestinal crypts by P7 and assume an adult duodenal–ileal distribution by P28 (Fig. 1*E*). Lysozyme is first detectable in nonproliferating epithelial (Paneth) cells located at the base of P10 crypts. Lysozyme appears 3 days after EF (P10 versus P7). The result is that >95% of Paneth cells, which first acquire the capacity to produce lysozyme at a given point along the duodenal–ileal axis, have already differentiated to a stage where they are able to coexpress EF and cryptdin.

The rates of epithelial cell proliferation and migration increase between the suckling and weaning periods, reaching an equilibrium state by P28, when the intestine completes its morphologic differentiation (19, 20). These events coincide with a dramatic increase in Paneth cell number and with a further evolution of the lineage's differentiation program. Changes in the levels of fucosylation of glycoconjugates produced by members of this lineage are readily detectable with fucose-specific lectins such as UEA-1, OPA, and AAA. Cryptdin-, EF-, and/or lysozyme-positive Paneth cells in jejunal crypts do not contain glycoconjugates detectable with UEA-1 in our *in situ* binding assay from the time of their first appearance at P7/10 through P14. By P21, strong granular staining by UEA-1 is evident (Fig. 1*D*). Acquisition of UEA-1 reactivity proceeds from P21 to P42 along the duodenal–ileal axis. Levels of sialylation are also altered during weaning. Sialylated epitopes detected by the lectin MAA appear in the granules of Paneth cells from P21 to P28 (Fig. 1*F*). Thus, the initial differentiation program of the Paneth cell lineage involves sequential expression of cryptdin → EF plus P/T → lysozyme → fucosylated and sialylated glycoconjugates.

Paneth Cell Differentiation in FVB/N Intestinal Isografts. Although qualitative and quantitative changes in the Paneth cell lineage can be linked temporally to crypt morphogenesis, the question arises as to the extent to which these changes reflect a cell-autonomous process versus the results of instructive interactions with other crypt epithelial and pericrypt mesenchymal populations, the evolving extracellular matrix, luminal contents, and/or hormones which are known to affect the differentiation programs of other lineages. Intestinal isografts were used to assess these possibilities. E15 gut undergoes region-appropriate morphologic differentiation of its endoderm when implanted under the subcutaneous tissues of young adult syngenic recipients, despite the fact that the isograft lacks a microflora and is not exposed to pancreatic and biliary secretions or a milk/chow diet (16). E15 FVB/N small intestinal and colonic isografts were implanted into P42 FVB/N male recipients and harvested 4–46 days later. The Paneth cell lineage is not detectable in colonic isografts at any stage of their development, just like the intact FVB/N colon. In contrast, there are several abnormalities in the small intestinal isografts. (*i*) Paneth cell development is accelerated: UEA-1-, EF-, and P/T-positive cells appear within 7–9 days after implantation (equivalent to P3–P5 intact small intestine) (Fig. 1*G*). (*ii*) The sequence of initial Paneth cell differentiation is disrupted. There is a

population of lysozyme-positive cells, first evident 9 days after implantation (equivalent to P5 intact gut), which do not contain detectable levels of EF or cryptdin. Likewise, there are populations of EF-positive cells which do not contain cryptdin and cryptdin-positive cells which do not contain EF. This finding contrasts with the observation that when lysozyme-positive Paneth cells first appear in the crypts of the intact P10 gut, they coexpress these other markers. (*iii*) The duodenal/ileal ratio of crypts with Paneth cells is greater in P3, P5, and P7 isografts than in the comparably aged intact FVB/N gut. These regional perturbations reflect the precocious differentiation/maturation of the Paneth cell lineage in "P3–P7" isografts (Fig. 1*H*). The proximal–distal gradient in Paneth distribution subsequently evolves in an appropriate temporal as well as spatial fashion in P14–P42 small intestinal isografts. (*iv*) Full granular staining of Paneth cells with UEA-1 is achieved by P5 in the isografts but only by P25 in the intact FVB/N gut. The E15 isograft is exposed to an adult hormonal milieu once it is implanted into the P42 host. The four abnormalities appear regardless of the gender of the recipient host, suggesting that androgens do not play a primary role. The enterocyte-specific brush-border hydrolase sucrase–isomaltase (SI) can be precociously induced during gut development by administering glucocorticoids. SI normally appears in FVB/N jejunal villi by P25. However, immunoreactive SI is evident in the isografts by P10 (data not shown). These findings raise the possibility that glucocorticoids (or other hormonal factors) may modulate some of the developmental changes in Paneth cell differentiation, proliferation, and distribution noted in the normal mouse gut (21).

Paneth Cell Differentiation in the Developing Intestine of Germ-Free, Ex-Germ-Free, and Conventional NMRI Mice. Cryptdin-positive cells are apparent at P1 in germ-free and conventional NMRI mice and have a distribution similar to that noted in FVB/N mice of comparable age. However, lysozyme-producing Paneth cells are first detectable at P14 in germ-free animals, compared with P10 in conventional NMRI mice. Differences in the number and distribution of lysozyme-positive Paneth cells disappear at the time of weaning (P21–P25). The lectin panel revealed no alterations in glycosylation between Paneth cells in germ-free and conventional mice except for expression of the terminal α-fucosylated epitopes recognized by AAA: Paneth cells in P28–P42 germ-free NMRI mice exhibit strong staining of their apical granules and cytoplasm, whereas Paneth cells in conventional P28–P42 NMRI mice have little to no AAA staining. When P28 germ-free NMRI mice are conventionalized and sacrificed 2 weeks later, the resulting P42 "ex-germ-free" mice demonstrate little to no Paneth cell staining with AAA—i.e., they are equivalent to P42 mice who have had a normal gut flora since birth. These analyses indicate that establishment of the Paneth cell lineage in the developing mouse intestine can proceed in the absence of microflora with only modest alterations in its differentiation program.

Cellular Patterns of Expression of a Cryptdin 2(−6500 to +34)/hGH(+3) Transgene in Developing and Adult FVB/N Mice. We linked nt −6500 to +34 of the mouse cryptdin 2 gene to the hGH gene beginning at its nt +3 and used this construct to generate several lines of transgenic mice. The cryptdin 2(−6500 to +34) and hGH(+3) segments were selected for several reasons. In the adult mouse, cryptdin 2 expression is confined to small intestinal Paneth cells, with highest steady-state levels of mRNA in jejunum and ileum (22). Moreover, nt −6500 to +1 of cryptdin 2 include regions

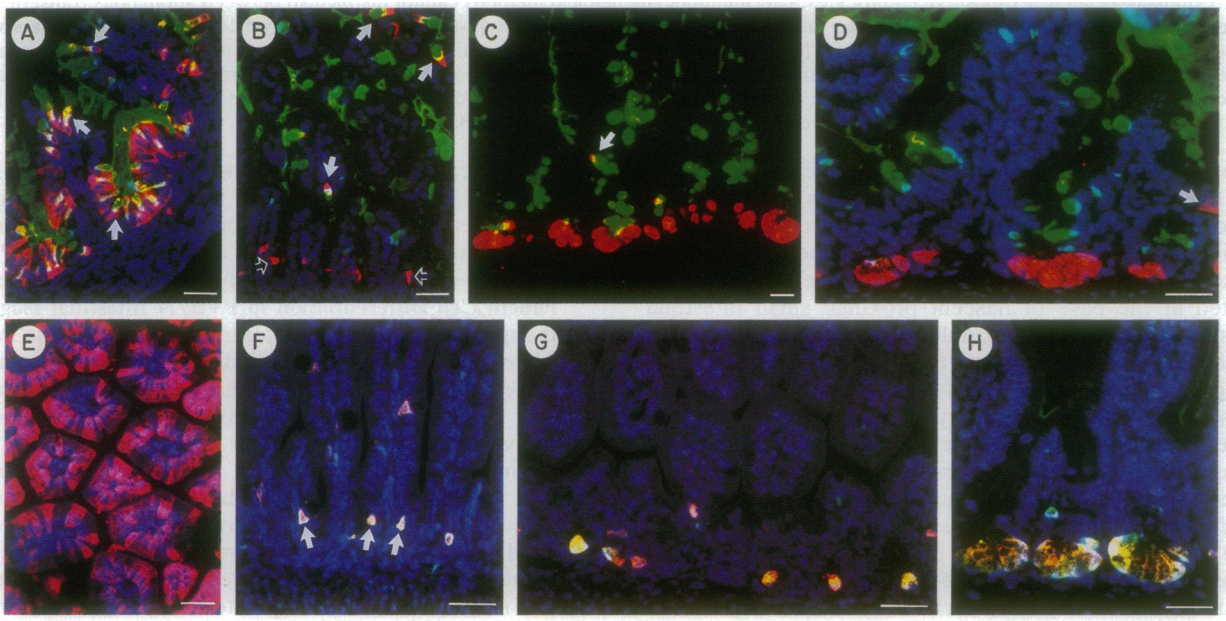

FIG. 2. Patterns of expression of the cryptdin 2(−6500 to +34)/hGH(+3) transgene in mice of line 61. (*A*) Ileum at P1 stained with goat anti-hGH and indocarbocyanine-tagged donkey anti-goat immunoglobulins (red–magenta), FITC-conjugated UEA-1 (green), and Hoescht nuclear stain (blue). Most cells in the intervillus epithelium (located in the lower portion of the micrograph) produce hGH (red–magenta). A subset of these hGH-positive cells bind UEA-1 (green–yellow when colocalized with hGH; arrows). (*B*) Ileum at P5 stained as in *A*. hGH persists at the base of the nascent crypts (red-colored cells; open arrows). Solid arrows point to members of the subset of UEA-1-positive goblet cells, located in the crypts and lower portions of associated villi, that express hGH. (*C*) Ileum at P14 stained as in *A*, but without Hoescht stain. Arrow points to a hGH-positive goblet cell. (*D*) Ileum at P42, stained as in *A*. hGH staining is restricted largely to Paneth cells (red). Arrow indicates a rare hGH-positive cell in the lamina propria. These rare cells do not coexpress lysozyme or IgA. (*E*) Ileal villi at P1, stained as in *A* but without UEA-1. Villi have been sectioned perpendicular to their basilar–apical axis. Note the extensive hGH staining of enterocytes and goblet cells. (*F*) P5 proximal small intestine stained with anti-hGH and Hoescht dye as in *A*, plus rabbit anti-cryptdin and FITC-labeled donkey anti-rabbit immunoglobulins. Arrows point to cells located at the base of crypts that coexpress hGH and cryptdin. Villus-associated goblet cells that coexpress hGH and cryptdin are also apparent (light pink). (*G*) Cryptdin/hGH colocalization in cells located at the base of P14 jejunal crypts (yellow–pink). The section was stained as in *F*. (*H*) Cryptdin/hGH colocalization in Paneth cells (yellow–brown) of P42 ileal crypts. (Bars = 25 μm.)

of high homology to the 5′ nontranscribed domains of three other genes encoding Paneth cell-specific mouse cryptdins (cryptdins 1, 3, and 5) (data not shown). Finally, production of hGH in proliferating and nonproliferating crypt epithelial cells has no apparent effect on the differentiation programs of the intestine's four lineages (11).

Four pedigrees were studied. Mice belonging to line 61 express the transgene from E18 through at least P180. Blot hybridization and reverse transcription–PCR analyses of RNA prepared from stomach, small intestine, cecum, colon, and 11 other organs from P42 line 61 mice indicates that, like cryptdin mRNA, hGH mRNA is confined to the small intestine, with higher levels in jejunum/ileum than in duodenum. Members of lines 70, 57, and 38 display a progressive extinction of intestinal transgene expression with increasing age. In line 57, expression disappears by P10. In line 38, expression begins to dissipate by P21 and is extinguished by P42. In line 70, reporter expression is virtually identical to that noted in line 61 up to P21 but then declines so that by P42, hGH mRNA is only detectable in the small bowel by reverse transcription–PCR assays. Despite these temporal differences, the cell lineage-specific and regional patterns of the transgene expression in the intestinal epithelium are the same in all four pedigrees at those stages of development where comparisons are possible.

At E18, the proximal intestine of transgenic animals contains villi with scattered hGH-producing enterocytes and goblet cells. A more abundant population of hGH-positive cells is present in the intervillus epithelium. Greater numbers of hGH-positive, villus-associated, columnar epithelial cells can be found in the distal small intestine. As in the proximal intestine, the majority of hGH-positive cells reside in the intervillus epithelium. At P1, hGH is produced in proliferating and nonproliferating cells in the proximal small intestine's intervillus epithelium as well as in a subpopulation of goblet cells (both UEA-1 positive and negative). The intervillus and villus-associated epithelium stains for hGH in the distal gut (Fig. 2 *A* and *E*). Most of these hGH-positive cells do not coexpress cryptdin, though all cryptdin-positive cells produce hGH. The pattern of transgene expression in the intervillus epithelium remains unchanged through P5 (Fig. 2 *B* and *F*). Between P5 and P7, hGH becomes restricted to a subpopulation of cells at the base of nascent crypts. These cells possess apical secretory granules and are BrdUrd-negative. Greater than 95% coexpress cryptdin. A small population of villus-associated goblet cells contain hGH (Fig. 2*B*). By P14, hGH production is largely limited to nonproliferating, cryptdin-positive Paneth cells in duodenal, jejunal, and ileal crypts (Fig. 2 *C* and *G*). By P28–42, >95% of hGH-positive cells located at the base of crypts coexpress EF, lysozyme, and/or UEA-1 (e.g., Fig. 2 *D* and *H*). At P42, duodenal–ileal variations in the number of hGH-positive crypts and number of hGH-positive cells per crypt mimic regional variations in the number of cryptdin-immunoreactive crypts/cells. While cryptdin-producing goblet cells are readily detectable up to P5–7 in normal FVB/N mice, expression of hGH in goblet cells continues through P42. However, they are found only in the distal gut and number <1 cell per 50 villi. None coexpress cryptdin, although some do bind UEA-1. Expression of the transgene in a subpopulation of goblet cells again raises the question whether Paneth cells and at least a subpopulation of goblet cells are descended from a common transit-cell progenitor (3).

Comparisons of transgenic mice and their normal littermates indicated that the hGH reporter has no discernible effect on the patterns of cryptdin, EF, lysozyme, or glycoconjugate expression in Paneth cells or on the patterns of lectin binding to members of the other three gut epithelial cell lineages distributed along the crypt–villus axis.

Prospectus. Given its inappropriate expression in a large population of proliferating and nonproliferating cells through P5 and its subsequent restriction to the Paneth cell lineage during the time of crypt purification, the cryptdin 2(−6500 to +34)/hGH(+3) transgene may be a useful tool for analyzing crypt morphogenesis and its relationship to the evolution of the Paneth cell lineage. Cryptdin 2(−6500 to +34) represents the starting point for additional promoter mapping studies to identify cis-acting elements that control Paneth cell-specific gene expression. It should also be useful for conducting gain-of-function or loss-of-function experiments. The strategic location of Paneth cells just below the stem-cell zone, together with their apical secretory apparatus, provides a unique opportunity for introducing (injecting) foreign gene products into the crypt and assessing their effects on gut epithelial cell biology at various stages of development. The functional significance of Paneth cells could be evaluated through lineage-ablation with an attenuated diphtheria toxin (23). Cryptdin 2(−6500 to +34) linked to this or other reporters could be used to further define the lineage interrelationships of Paneth cells. Finally, conditionally immortalized Paneth cell lines could be generated from transgenic mice containing these promoter elements linked to a temperature-sensitive, mutant simian virus 40 large tumor antigen (24).

We thank Mike Selsted, Rita Mulherkar, and Peter Traber for gifts of anti-cryptdin, anti-EF, and anti-sucrase–isomaltase sera, respectively. This work was supported by grants from the National Institutes of Health (DK37960, DK44632), Amgen, and the Swedish Medical Research Council (16X-06852).

1. Gordon, J. I., Schmidt, G. H. & Roth, K. A. (1992) *FASEB J.* **6**, 3039–3050.
2. Troughton, J. & Trier, J. S. (1969) *J. Cell Biol.* **41**, 257–269.
3. Cheng, H. (1974) *Am. J. Anat.* **141**, 521–536.
4. Raaberg, L., Nexo, E., Damsgaard, J. & Poulsen, S. (1988) *Histochemistry* **89**, 351–356.
5. DeSauvage, F. J., Keshav, S., Kuang, W., Gillett, N., Henzel, W. & Goeddel, D. V. (1992) *Proc. Natl. Acad. Sci. USA* **89**, 9089–9093.
6. Mulherkar, R., Desai, S. J., Rao, R. S., Wagle, A. S. & Deo, M. G. (1991) *Histochemistry* **96**, 371–374.
7. Calvert, R. & Pothier, P. (1990) *Anat. Rec.* **227**, 199–206.
8. Schmidt, G. H., Winton, D. J. & Ponder, B. A. J. (1988) *Development (Cambridge, U.K.)* **103**, 785–790.
9. Loeffler, M., Birke, A., Winton, D. J. & Potten, C. (1993) *J. Theor. Biol.* **160**, 471–491.
10. Granholm, T., Froysa, B., Lundstrom, C., Wahab, A., Midtvedt, T. & Soder, O. (1992) *Cytokinetics* **4**, 545–550.
11. Simon, T. C., Roth, K. A. & Gordon, J. I. (1993) *J. Biol. Chem.* **268**, 18345–18358.
12. Roth, K. A., Hertz, J. M. & Gordon, J. I. (1990) *J. Cell Biol.* **110**, 1791–1801.
13. Selsted, M. E., Miller, S. I., Henschen, A. H. & Ouellette, A. J. (1992) *J. Cell Biol.* **118**, 929–936.
14. Markowitz, A. J., Wu, G. D., Birkenmeier, E. H. & Traber, P. G. (1993) *Am. J. Physiol.* **265**, G526–G539.
15. Falk, P., Roth, K. A. & Gordon, J. I. (1994) *Am. J. Physiol.* **266**, G987–G1003.
16. Huttner, K. M., Selsted, M. E. & Ouellette, A. J. (1994) *Genomics* **19**, 448–453.
17. Ouellette, A. J., Hsieh, M. M., Nosek, M. T., Cano-Gauci, D. F., Huttner, K. M., Buick, R. N. & Selsted, M. E. (1994) *Infect. Immun.*, in press.
18. Mulherkar, R., Desai, S. J., Rao, R. S., Wagle, A. S. & Deo, M. G. (1993) *FEBS Lett.* **317**, 263–266.
19. Al-Nafussi, A. I. & Wright, N. A. (1982) *Virch. Arch. Cell Pathol.* **40**, 51–62.
20. Cheng, H. & Bjerknes, M. (1985) *Anat. Rec.* **211**, 420–426.
21. Dinsdale, D. & Biles, B. (1986) *Cell Tissue Res.* **246**, 183–187.
22. Ouellette, A. J., Greco, R. M., James, M., Frederick, D., Naftilan, J. & Fallon, J. T. (1989) *J. Cell Biol.* **108**, 1687–1695.
23. Breitman, M. L., Rombola, H., Maxwell, I. H., Klintworth, G. K. & Bernstein, A. (1990) *Mol. Cell. Biol.* **10**, 474–479.
24. Whitehead, R. H., VanEeden, P. E., Noble, M. D., Ataliotis, P. & Jat, P. S. (1993) *Proc. Natl. Acad. Sci. USA* **90**, 587–591.